LETTER

doi:10.1038/nature09425

Late middle Eocene epoch of Libya yields earliest known radiation of African anthropoids

Jean-Jacques Jaeger[1], K. Christopher Beard[2], Yaowalak Chaimanee[3], Mustafa Salem[4], Mouloud Benammi[1], Osama Hlal[4], Pauline Coster[1], Awad A. Bilal[5], Philippe Duringer[6], Mathieu Schuster[1], Xavier Valentin[1], Bernard Marandat[7], Laurent Marivaux[7], Eddy Métais[8], Omar Hammuda[4] & Michel Brunet[1,9]

Reconstructing the early evolutionary history of anthropoid primates is hindered by a lack of consensus on both the timing and biogeography of anthropoid origins[1–3]. Some prefer an ancient (Cretaceous) origin for anthropoids in Africa or some other Gondwanan landmass[4], whereas others advocate a more recent (early Cenozoic) origin for anthropoids in Asia[1,2,5], with subsequent dispersal of one or more early anthropoid taxa to Africa. The oldest undoubted African anthropoid primates described so far are three species of the parapithecid *Biretia* from the late middle Eocene Bir El Ater locality of Algeria[6] and the late Eocene BQ-2 site in the Fayum region of northern Egypt[7]. Here we report the discovery of the oldest known diverse assemblage of African anthropoids from the late middle Eocene Dur At-Talah escarpment in central Libya. The primate assemblage from Dur At-Talah includes diminutive species pertaining to three higher-level anthropoid clades (Afrotarsiidae, Parapithecidae and Oligopithecidae) as well as a small species of the early strepsirhine primate *Karanisia*. The high taxonomic diversity of anthropoids at Dur At-Talah indicates either a much longer interval of anthropoid evolution in Africa than is currently documented in the fossil record or the nearly synchronous colonization of Africa by multiple anthropoid clades at some time during the middle Eocene epoch.

The chronology and biogeography of anthropoid origins have long been debated[1–7]. Molecular estimates of anthropoid origins typically advocate an early origin for the group, often extending back to the late Cretaceous[8]. In contrast, palaeontological data generally support a Cenozoic origin for anthropoids, although a wide range of potential origination dates have been suggested on the basis of fossils, of ages ranging from Palaeocene to later Eocene[1]. Similarly, there is no current consensus on where anthropoids originated. Since the discovery of a series of diverse anthropoid faunas in the Fayum region of Egypt, it has often been assumed that Africa was the birthplace of the anthropoid clade[9–11]. This interpretation has been challenged by the discovery of multiple taxa of basal anthropoids in Asia[5,12–15] and the recent finding that the putative early or middle Eocene African anthropoid *Algeripithecus* is actually a strepsirhine[16]. With the possible exception of the enigmatic *Altiatlasius koulchii* from the late Palaeocene epoch of Morocco[17], the oldest African anthropoids acknowledged so far come from the late middle Eocene (about 40 Myr ago) Bir El Ater locality in Algeria[6]. Here we augment the record of African anthropoids from the late middle Eocene on the basis of a new micromammal assemblage from Dur At-Talah in central Libya (Fig. 1). This fauna includes a small-bodied strepsirhine and a diversity of basal anthropoids, including primitive representatives of Afrotarsiidae, Parapithecidae and Oligopithecidae. The age and diversity of the Dur At-Talah primate fauna indicates substantial gaps in either the African or the Asian fossil record of anthropoid evolution (and possibly both).

The Dur At-Talah escarpment was first explored palaeontologically during the second half of the twentieth century[18]. This early phase of exploration yielded a vertebrate fauna mainly composed of taxa having medium to large body size, such as the early proboscideans *Barytherium grave*, *Arcanotherium savagei* and *Moeritherium chehbeurameuri*. Our recent fieldwork at Dur At-Talah has focused on enhancing the vertebrate record from this region by concentrating on the previously neglected microfauna. In addition to the primates reported here, five taxa of phiomyid rodents have been identified so far[19]. Biostratigraphic correlation based mainly on rodents and proboscideans suggests that the Dur At-Talah fauna approximates that from Bir El Ater in Algeria[19], which is regarded as late middle Eocene[20,21]. This correlation is supported by the new data from fossil primates described here. Available biostratigraphic evidence is also consistent with palaeomagnetic data from the Dur At-Talah section, which suggest correlation with Chron 18n.1n (38–39 Myr ago; late Bartonian)[19]. Specimens described here are housed in the palaeontological collections of Al Fateh University (Tripoli, Libya).

Primates Linnaeus, 1758
Strepsirhini Geoffroy, 1812
Lorisiformes Gregory, 1915
Karanisia Seiffert *et al.*, 2003
Karanisia arenula, sp. nov.

Holotype. DT1-42, left M_2 (Fig. 2e).
Horizon and locality. DT-Loc.1, Bioturbated Unit, Bartonian Dur At-Talah escarpment, central Libya[19].
Diagnosis. Differs from *Karanisia clarki*[22] in being smaller (adult body mass is estimated at 120–132 g). For hypodigm, description and metrics, see Supplementary Information.
Etymology. arena (Latin): sand, refers to the sandy matrix that yielded the hypodigm; -ula (Latin): diminutive suffix, in allusion to the small size of this species.

Anthropoidea Mivart, 1864
Afrotarsiidae Ginsburg and Mein, 1987
Afrotarsius Simons and Bown, 1985
Afrotarsius libycus, sp. nov.

Holotype. DT1-35, left M_1 or M_2 (Fig. 2k, l).
Horizon and locality. DT-Loc.1, Bioturbated Unit, Bartonian Dur At-Talah escarpment, central Libya[19].
Diagnosis. Differs from *Afrotarsius chatrathi*[23] in having narrower lower molars bearing hypoconid and entoconid cusps that are less isolated and less spire-like. Hypoconulid of M_1 or M_2 projects farther distally than in *A. chatrathi*. Adult body mass estimated at 130–232 g. For hypodigm, description and metrics, see Supplementary Information.
Etymology. Refers to the provenance of this species.

[1]Institut International de Paléoprimatologie et Paléontologie humaine, Évolution et Paléoenvironnements, CNRS UMR 6046, Université de Poitiers, 40 Avenue du Recteur Pineau, 86022 Poitiers, France. [2]Section of Vertebrate Paleontology, Carnegie Museum of Natural History, 4400 Forbes Avenue, Pittsburgh, Pennsylvania 15213 USA. [3]Paleontology Section, Department of Mineral Resources, Rama VI Road, Bangkok 10400, Thailand. [4]Geology Department, Al Fateh University, Tripoli, Libya. [5]Geology Department, Garyounis University, Benghazi, Libya. [6]Institut de Physique du Globe de Strasbourg, CNRS/Université de Strasbourg UMR 7516, Institut de Géologie, 1 rue Blessig, 67084 Strasbourg, France. [7]Institut des Sciences de l'Évolution, CNRS UMR 5554, Université Montpellier II, Place E. Bataillon, 34095 Montpellier, France. [8]Groupe 'TOTAL', 2 Place J. Millier, la Défense 6, 92400 Courbevoie, France. [9]Chaire de Paléontologie Humaine, Collège de France, Place M. Berthelot, 75005 Paris, France.

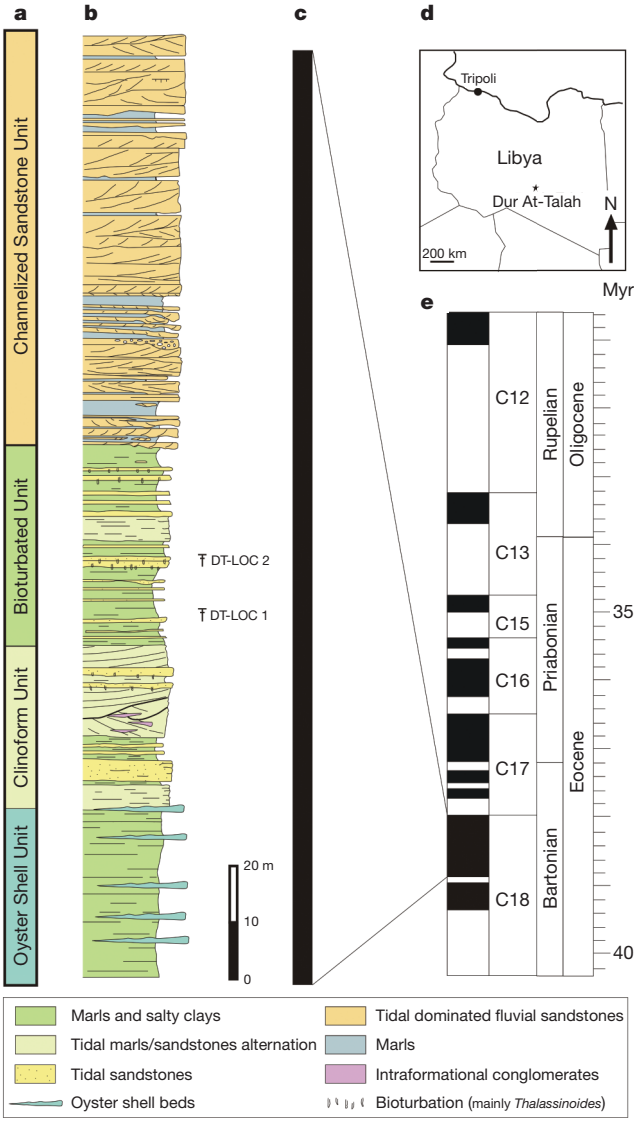

Figure 1 | Stratigraphy and correlation of the Dur At-Talah section. **a**, Stratigraphic units[19]. **b**, Lithology and sedimentology of the section. **c**, Local magnetic polarity stratigraphy (black bar indicates zone of normal polarity). **d**, Map of Libya showing the geographic position of the Dur At-Talah escarpment. **e**, Preferred correlation to the Geomagnetic Polarity Time Scale[19,29].

Parapithecidae Schlosser, 1911
Biretia piveteaui de Bonis *et al.*, 1988

Referred material. DT1-26, left M^1; DT1-27, right M^2; DT1-28, right M^3; DT1-29, left M_3; DT2-23, right M^3; DT2-24, right M_2 (Fig. 2q–w).
Horizon and locality. DT-Loc.1 and DT-Loc.2, Bioturbated Unit, Bartonian Dur At-Talah escarpment, central Libya[19].
Emended diagnosis. *Biretia piveteaui*[6] (adult body mass estimated at 292–470 g) is larger than *B. fayumensis*. M^{1-2} differ from those of *B. fayumensis*[7] and *B. megalopsis*[7] in having more isolated metaconules lacking any connection with either the protocone or the metacone. M^3 mesiodistally shorter than that of *B. megalopsis*. M^3 with smaller metacone and less extensive trigon lacking metaconule, in contrast to that of *B. megalopsis*. For description and metrics, see Supplementary Information.

Oligopithecidae Simons, 1989
Talahpithecus parvus, gen. et sp. nov.

Holotype. DT1-31, left M^1 or M^2 (Fig. 2n).
Horizon and locality. DT-Loc.1, Bioturbated Unit, Bartonian Dur At-Talah escarpment, central Libya[19].
Diagnosis. Smaller (adult body mass estimated at 226–376 g) than *Catopithecus* and *Oligopithecus*. Upper molars without mesostyle and with smaller hypocone than in *Catopithecus*. Crests surrounding upper molar trigon more trenchant than in *Oligopithecus* and *Catopithecus*. Lower molars with relatively narrower talonid and higher trigonid with more nearly vertical postvallid than in *Oligopithecus* and *Catopithecus*. For hypodigm, description and metrics, see Supplementary Information.
Etymology. talah (Arabic): tree, refers to the provenance of this genus; parvus (Latin): small, refers to the size of this species.

All four primate taxa currently known from Dur At-Talah are remarkably small, ranging from 120 to 470 g in estimated adult body mass. Such a small size distribution for the earliest known African radiation of anthropoids reinforces the conclusion drawn from analysis of the middle Eocene primate assemblage of Shanghuang, China, that the origin of anthropoids occurred at very small body size[24]. Indeed, if recent phylogenetic analyses recognizing oligopithecids as early members of the catarrhine clade are correct[7], the small size of *Talahpithecus parvus* would suggest that even the origin of crown anthropoids and the platyrrhine/catarrhine divergence occurred at small body mass. However, by the time of the late Eocene L-41 primate fauna from the Fayum region of Egypt[10], larger anthropoid taxa had begun to supplant these diminutive taxa, and this trend towards increasing body mass among early African anthropoids continued into the Oligocene epoch. The common occurrence of *Biretia piveteaui* at both Bir El Ater and Dur At-Talah supports a similar age for these faunas. The small size of *Karanisia arenula* from Dur At-Talah in comparison with *K. clarki* from BQ-2 in the Fayum, as well as the small size and primitive anatomy of *Talahpithecus parvus* in comparison with Fayum oligopithecids such as *Catopithecus browni*, reinforce biostratigraphic data from rodents and proboscideans suggesting that Dur At-Talah is roughly equivalent to Bir El Ater in age. Both of the latter faunas seem to be older than BQ-2 in the Fayum[19].

The phylogenetic affinities of three of the four primate taxa documented at Dur At-Talah are uncontroversial, but there is no current consensus regarding the broader affinities of *Afrotarsius*, represented at Dur At-Talah by *A. libycus*. Originally described as a possible African tarsiid (hence the generic name)[23], multiple subsequent authors have suggested that *Afrotarsius* is a basal member of the anthropoid clade[9,25,26]. The previously unknown upper-molar morphology of *Afrotarsius*, documented here, supports an attribution of this genus to Anthropoidea rather than Tarsiidae (or Tarsiiformes). Like those of Asian eosimiid anthropoids (*Eosimias*, *Phenacopithecus* and *Bahinia*)[5,14], the upper molars of *Afrotarsius* bear an elongated postmetacrista and an enlarged shelf-like structure buccal to the metacone. The upper molars of *Afrotarsius* and eosimiids also share transversely oriented crests that variably connect the paracone and metacone with their associated conules (or remnants thereof). The upper molars of *Afrotarsius* differ from those of eosimiids in retaining continuity between the postmetaconule crista and the postcingulum, which is lost in eosimiids. As noted by previous authors[25], M_3 of *Afrotarsius* is distinctively anthropoid-like (and differs from that of tarsiids) in having a remarkably abbreviated hypoconulid lobe (Fig. 2m). In view of these anatomical characters, we regard *Afrotarsius* as a relatively basal member of the anthropoid clade. However, substantial additional evidence will be required to ascertain how *Afrotarsius* relates to other early anthropoid taxa, particularly eosimiids. Dental similarities between *Afrotarsius* and tarsiids probably reflect the convergent acquisition of trenchant molar crests as an adaptation for insectivory.

The presence of three distinct clades of anthropoids (Afrotarsiidae, Parapithecidae and Oligopithecidae) in the late middle Eocene Dur At-Talah fauna is surprising, especially in view of the lower diversity of early anthropoids that has been described so far from the BQ-2 locality of late Eocene age in northern Egypt[7]. Recent comprehensive analyses of early anthropoid relationships disagree on many aspects of tree

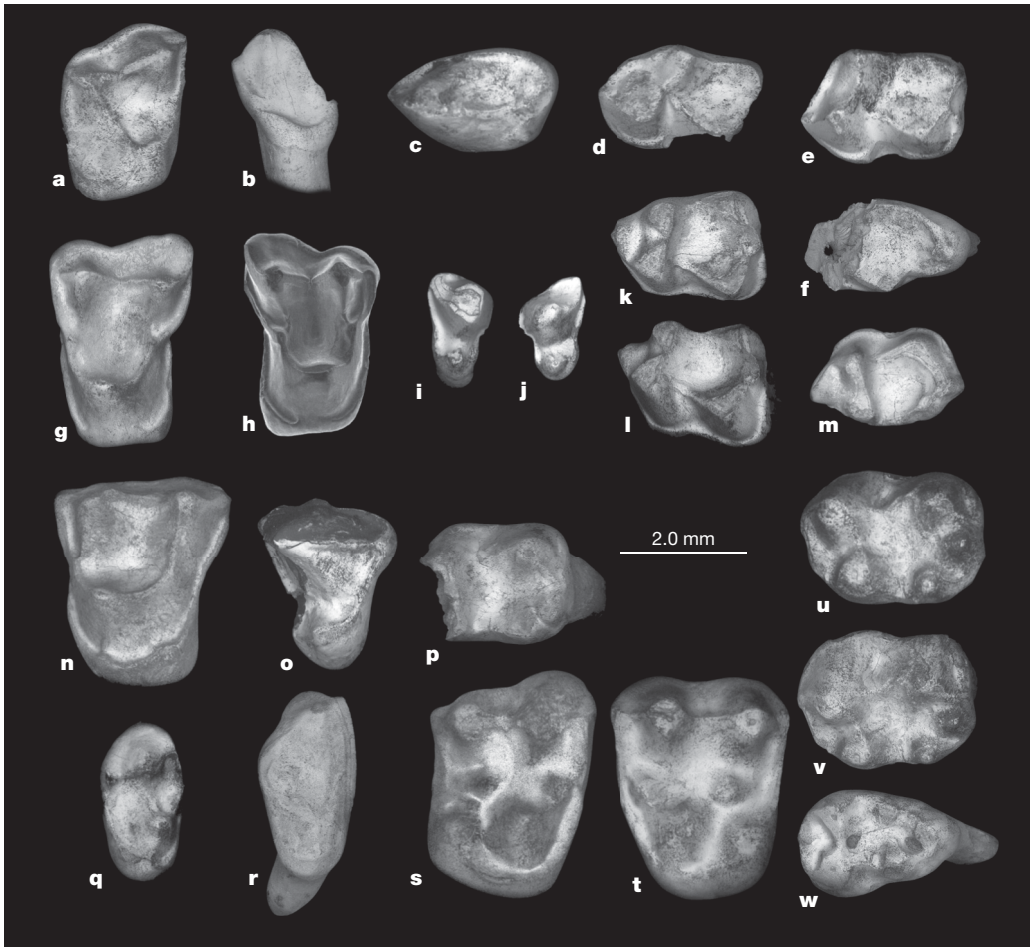

Figure 2 | Scanning electron microscope images of fossil primate teeth from Dur At-Talah. **a**–**f**, *Karanisia arenula* sp. nov. **a**, Right M^3 (DT1-37), occlusal view. **b**, Right P_3 (DT1-38), lingual view. **c**, Left P_4 (DT1-39), occlusal view. **d**, Left M_1 (DT1-41), occlusal view. **e**, Holotype left M_2 (DT1-42), occlusal view. **f**, Fragmentary left M_3 (DT1-43), occlusal view. **g**–**m**, *Afrotarsius libycus* sp. nov. **g**, Left M^2 (DT1-33), occlusal view. **h**, Right M^2 (DT1-34), occlusal view. **i**, Right P^3 (DT1-31), occlusal view. **j**, Left P^3 (DT1-32), occlusal view. **k**, Holotype left M_1 or M_2 (DT1-35), occlusal view. **l**, Holotype left M_1 or M_2 (DT1-35), oblique buccal view. **m**, Right M_3 (DT1-36), occlusal view. **n**–**p**, *Talahpithecus parvus* gen. et sp. nov. **n**, Holotype left M^1 or M^2 (DT1-31), occlusal view. **o**, Right P^4 (DT1-30), mesial oblique view. **p**, Fragmentary right M_1 or M_2 (DT1-32), occlusal view. **q**–**w**, *Biretia piveteaui*. **q**, Right M^3 (DT2-23), occlusal view. **r**, Right M^3 (DT1-28), occlusal view. **s**, Right M^2 (DT1-27), occlusal view. **t**, Left M^1 (DT1-26), occlusal view. **u**, Right M_2 (DT2-24), occlusal view. **v**, Right M_2 (DT2-24), oblique buccal view. **w**, Left M_3 (DT1-29), occlusal view.

topology[7,27], but all current reconstructions of early anthropoid phylogeny insist that the three anthropoid clades represented at Dur At-Talah occupy disparate positions on the evolutionary tree. The high degree of morphological, taxonomic and presumably ecological diversity apparent in the Dur At-Talah anthropoid fauna can be explained only by a substantial interval of earlier evolutionary history for this group. Given the apparent absence of anthropoids in significantly older, but reasonably well sampled, Eocene African localities such as Glib Zegdou in western Algeria[16], it seems doubtful that the 'missing' evolutionary history of the Dur At-Talah anthropoids can be explained simply by reference to the poorly sampled early Cenozoic fossil record of Africa. An alternative hypothesis that now demands serious consideration is that multiple Asian anthropoid clades may have colonized Africa more or less synchronously during the middle Eocene, alongside anomaluroid and hystricognathous rodents. In either case, further palaeontological exploration of middle Eocene localities in Africa and Asia will be necessary to illuminate this poorly documented interval of primate evolutionary history.

METHODS SUMMARY

Taxonomic allocation. Fossil specimens from Dur At-Talah were segregated into taxa on the basis of both metric and morphological compatibility. Specimens from Dur At-Talah were extensively compared with original specimens and casts of African and Asian fossil primates to establish the systematic affinities of the Dur At-Talah taxa.

Estimation of body mass. Mean estimates of adult body mass for each primate taxon from Dur At-Talah were obtained by using the regression equations provided by Conroy[28]. Conroy's regressions estimate body mass on the basis of M_1 area. This tooth locus is not definitively known for any of the Dur At-Talah anthropoid taxa, because M_1 and M_2 are not readily distinguished in *Afrotarsius* and because the sole lower molar currently known for *Talahpithecus parvus* is fragmentary (see Supplementary Information). In these cases, M_2 dimensions may have been substituted for M_1 (as was certainly the case for *Biretia piveteaui*). Two regression equations were used to estimate adult body mass for each primate taxon known from Dur At-Talah. Conroy's 'all primates' regression was used in every case, although more taxonomically restricted regressions were also employed (Conroy's 'prosimians' regression was used for *Karanisia*, and Conroy's 'monkeys' regression was used for the anthropoids).

Full Methods and any associated references are available in the online version of the paper at www.nature.com/nature.

Received 7 July; accepted 16 August 2010.

1. Beard, K. C. *The Hunt for the Dawn Monkey: Unearthing the Origins of Monkeys, Apes, and Humans* (Univ. California Press, Berkeley, 2004).
2. Beard, K. C. in *Primate Biogeography* (eds Lehman, S. G. & Fleagle, J. G.) 439–467 (Springer, 2006).
3. Williams, B. A., Kay, R. F. & Kirk, E. C. New perspectives on anthropoid origins. *Proc. Natl Acad. Sci. USA* **107,** 4797–4804 (2010).
4. Miller, E. R., Gunnell, G. F. & Martin, R. D. Deep time and the search for anthropoid origins. *Yearb. Phys. Anthropol.* **48,** 60–95 (2005).
5. Jaeger, J.-J. *et al.* A new primate from the middle Eocene of Myanmar and the Asian early origin of anthropoids. *Science* **286,** 528–530 (1999).

6. de Bonis, L., Jaeger, J.-J., Coiffait, B. & Coiffait, P.-E. Découverte du plus ancien primate catarrhinien connu dans l'Éocène supérieur d'Afrique du Nord. *C. R. Acad. Sci.* **306,** 929–934 (1988).
7. Seiffert, E. R. *et al.* Basal anthropoids from Egypt and the antiquity of Africa's higher primate radiation. *Science* **310,** 300–304 (2005).
8. Bininda-Emonds, O. R. P. *et al.* The delayed rise of present-day mammals. *Nature* **446,** 507–512 (2007).
9. Fleagle, J. G. & Kay, R. F. The phyletic position of the Parapithecidae. *J. Hum. Evol.* **16,** 483–532 (1987).
10. Simons, E. L. Diversity in the early Tertiary anthropoidean radiation in Africa. *Proc. Natl Acad. Sci. USA* **89,** 10743–10747 (1992).
11. Ciochon, R. L. & Gunnell, G. F. Chronology of primate discoveries in Myanmar: influences on the anthropoid origins debate. *Yearb. Phys. Anthropol.* **45,** 2–35 (2002).
12. Beard, K. C., Qi, T., Dawson, M. R., Wang, B.-Y. & Li, C.-K. A diverse new primate fauna from middle Eocene fissure-fillings in southeastern China. *Nature* **368,** 604–609 (1994).
13. Beard, K. C., Tong, Y.-S., Dawson, M. R., Wang, J.-W. & Huang, X.-S. Earliest complete dentition of an anthropoid primate from the late middle Eocene of Shanxi Province, China. *Science* **272,** 82–85 (1996).
14. Beard, K. C. & Wang, J.-W. The eosimiid primates (Anthropoidea) of the Heti Formation, Yuanqu Basin, Shanxi and Henan Provinces, People's Republic of China. *J. Hum. Evol.* **46,** 401–432 (2004).
15. Beard, K. C. *et al.* A new primate from the Eocene Pondaung Formation of Myanmar and the monophyly of Burmese amphipithecids. *Proc. R. Soc. Lond. B* **276,** 3285–3294 (2009).
16. Tabuce, R. *et al.* Anthropoid versus strepsirhine status of the African Eocene primates *Algeripithecus* and *Azibius*: craniodental evidence. *Proc. R. Soc. Lond. B* **276,** 4087–4094 (2009).
17. Sigé, B., Jaeger, J.-J., Sudre, J. & Vianey-Liaud, M. *Altiatlasius koulchii* n. gen. et sp., primate omomyidé du Paléocène supérieur du Maroc, et les origines des euprimates. *Palaeontographica A* **214,** 31–56 (1990).
18. Wight, A. W. R. in *The Geology of Libya* Vol. 1 (eds Salem, M. J. & Busrewil, M. T.) 309–325 (Academic, 1980).
19. Jaeger, J.-J. *et al.* New rodent assemblages from the Eocene Dur At-Talah escarpment (Sahara of central Libya): systematic, biochronological, and palaeobiogeographical implications. *Zool. J. Linn. Soc.* **160,** 195–213 (2010).
20. Tabuce, R., Coiffait, B., Coiffait, P.-E., Mahboubi, M. & Jaeger, J.-J. A new species of *Bunohyrax* (Hyracoidea, Mammalia) from the Eocene of Bir el Ater (Algeria). *C. R. Acad. Sci.* **331,** 61–66 (2000).
21. Tabuce, R., Coiffait, B., Coiffait, P.-E., Mahboubi, M. & Jaeger, J.-J. A new genus of Macroscelidea (Mammalia) from the Eocene of Algeria: a possible origin for elephant-shrews. *J. Vertebr. Paleontol.* **21,** 535–546 (2001).
22. Seiffert, E. R., Simons, E. L. & Attia, Y. Fossil evidence for an ancient divergence of lorises and galagos. *Nature* **422,** 421–424 (2003).
23. Simons, E. L. & Bown, T. M. *Afrotarsius chatrathi*, first tarsiiform primate (?Tarsiidae) from Africa. *Nature* **313,** 475–477 (1985).
24. Gebo, D. L., Dagosto, M., Beard, K. C. & Qi, T. The smallest primates. *J. Hum. Evol.* **38,** 585–594 (2000).
25. Ginsburg, L. & Mein, P. *Tarsius thailandica* nov. sp., premier Tarsiidae (Primates, Mammalia) fossile d'Asie. *C. R. Acad. Sci.* **304,** 1213–1215 (1987).
26. Beard, K. C. A new genus of Tarsiidae (Mammalia: Primates) from the middle Eocene of Shanxi Province, China, with notes on the historical biogeography of tarsiers. *Bull. Carnegie Mus. Nat. Hist.* **34,** 260–277 (1998).
27. Kay, R. F., Williams, B. A., Ross, C. F., Takai, M. & Shigehara, N. in *Anthropoid Origins: New Visions* (eds Ross, C. F. & Kay, R. F.) 91–135 (Kluwer/Plenum, 2004).
28. Conroy, G. C. Problems of body-weight estimation in fossil primates. *Int. J. Primatol.* **8,** 115–137 (1987).
29. Gradstein, F. M., Ogg, J. G. & Smith, A. G. *A Geological Time Scale 2004* (Cambridge Univ. Press, 2004).

Supplementary Information is linked to the online version of the paper at www.nature.com/nature.

Acknowledgements This work has been completed under the framework of a cooperative programme between the University of Poitiers and Al Fateh University. Logistic and travel arrangements were provided by Al Fateh University. Financial support came from the University of Poitiers, from the CNRS 'Eclipse2' program and the ANR-05-BLAN-0235 and ANR-09-BLAN-0238-02-EVAH programs, from the Groupe 'TOTAL' and from a National Science Foundation grant to K.C.B. Scanning electron microscope images were produced by M. Bordes. Figures were designed by S. Riffaut and M. Klingler.

Author Contributions M.Br., M.Sa., O.H. and J.-J.J. designed and organized the project. J.-J.J., Y.C., X.V., M.Be., M.S., A.A.B., B.M. and L.M. collected palaeontological data. M.Be., P.C., M.Sch, O.Hl, P.D. and E.M. collected geological and palaeomagnetic data. J.-J.J., Y.C. and K.C.B. analysed the data. J.-J.J. and K.C.B. wrote the manuscript.

Author Information Reprints and permissions information is available at www.nature.com/reprints. The authors declare no competing financial interests. Readers are welcome to comment on the online version of this article at www.nature.com/nature. Correspondence and requests for materials should be addressed to J.-J.J. (jean-jacques.jaeger@univ-poitiers.fr)

METHODS

Taxonomic allocation. Fossil specimens from Dur At-Talah were segregated into taxa on the basis of both metric and morphological compatibility. The following taxa of Eocene–Oligocene primates from Africa and Asia formed the comparative sample used to make taxonomic decisions regarding the Dur At-Talah primates: *Karanisia clarki*, *Saharagalago misrensis*, *Tarsius eocaenus*, *Xanthorhysis tabrumi*, *Afrotarsius chatrathi*, *Eosimias sinensis*, *E. centennicus*, *E. dawsonae*, *Phenacopithecus krishtalkai*, *P. xueshii*, *Bahinia pondaungensis*, *Biretia piveteaui*, *B. fayumensis*, *B. megalopsis*, *Qatrania wingi*, *Arsinoea kallimos*, *Serapia eocaena*, *Proteopithecus sylviae*, *Catopithecus browni*, *Oligopithecus rogeri*.

Measurements. Standard measurements (mesiodistal length, buccolingual width; separate width measurements for lower molar trigonids and talonids) were obtained for each tooth in the current sample (Supplementary Table 1). Measurements were taken to the nearest 0.01 mm with digital calipers. Equivalent dimensions were estimated in the case of two fragmentary specimens (DT1-32 and DT1-43).

Body mass estimation. Estimates of adult body mass for each primate taxon from Dur At-Talah were obtained by using the regression equations provided by Conroy[28]. Conroy's regressions estimate body mass on the basis of M_1 area. For *Karanisia arenula* body mass was estimated from the mean M_1 area of the two available specimens (DT1-40 and DT1-41). Two estimates of the adult body mass of *Karanisia arenula* were obtained, using Conroy's 'all primates' and 'prosimians' regressions, respectively. The body mass of *Afrotarsius libycus* was estimated from the dimensions of the holotype lower molar (DT1-35), which is either an M_1 or an M_2. The body mass of *Biretia piveteaui* was estimated on the basis of DT2-24, regarded here as an M_2. These teeth do not differ appreciably in size in *Afrotarsius chatrathi*[23] and Fayum species of *Biretia*[7], suggesting that any error introduced by substituting the dimensions of M_2 for those of M_1 here is negligible. Body mass of *Talahpithecus parvus* was assessed on the basis of DT1-32, a fragmentary M_1 or M_2 whose length can only be estimated because of breakage. Two estimates of the adult body mass of each of the three anthropoid taxa represented at Dur At-Talah were obtained, using Conroy's 'all primates' and 'monkeys' regressions, respectively.

doi:10.1038/nature09425

Primates Linnaeus, 1758

Strepsirhini Geoffroy, 1812

Lorisiformes Gregory, 1915

Karanisia Seiffert et al., 2003

Karanisia arenula, sp. nov. (Fig. 2a-f)

Hypodigm. In addition to the holotype; DT1-37, right M^3; DT1-38, right P_3; DT1-39, left P_4; DT1-40, left M_1; DT1-41, left M_1; DT1-43, left M_3.

Description. DT1-38 (Fig. 2b) is interpreted as a right P_3 of *K. arenula*, although the tooth is single-rooted. This apparently conflicts with the condition in *K. clarki*, in which two alveoli have been identified as pertaining to this locus (see figure 1b in reference 22). The crown is simply constructed and mesially canted. The trigonid bears a single cusp, the protoconid, which is a buccolingually compressed cusp that is buccally convex. The lingual surface of the trigonid is unevenly excavated, with two roughly triangular invaginated areas being separated by a vertical ridge running from the lingual side of the protoconid towards the lingual cingulid. A short preprotocristid descends the mesial face of the protoconid. Where the latter structure meets the lingual cingulid, a tiny cuspule is present. The postprotocristid follows a more nearly vertical trajectory as it descends the distal side of the protoconid. It terminates just prior to reaching the short, simple talonid heel.

DT1-39 (Fig. 2c), a left P_4, is referred to *K. arenula* on the basis of its close morphological similarity to this tooth in *K. clarki*. The crown is double-rooted, and the talonid is longer than that of DT1-38, but otherwise these teeth are very similar (which is the chief reason why the latter tooth is identified as a P_3 of the same taxon). The trigonid is dominated by the buccolingually compressed protoconid, which is convex buccally and unevenly excavated lingually. Pre- and postprotocristids define the leading and distal edges of the trigonid. The more distal excavated area on the lingual surface of the trigonid is continuous with the talonid, which slopes lingually from the postprotocristid and hypoconid to the lingual cingulid, which is complete. Unlike that of *K. clarki*, P_4 in *K. arenula* lacks a complete buccal cingulid.

Aside from being significantly smaller, the lower molars of *K. arenula* generally resemble those of *K. clarki*. Only the holotype is complete and unbroken, so the following description is based on DT1-42, a left M_2 (Fig. 2e). The trigonid is rhomboidal in occlusal view, because the metaconid is shifted distally well beyond the level of the protoconid, giving the protocristid a distinctly oblique orientation. The trigonid as a whole is mesiodistally compressed, and the leading edge of the trigonid runs roughly parallel to the postcristid. The protoconid and metaconid are similar in height, but the paraconid is diminutive (DT1-42) or vestigial (DT1-41). A mesially directed crest defines the buccal margin of the trigonid, connecting the protoconid with the tiny paraconid. The talonid basin is also rhomboidal, because the postcristid runs roughly parallel to the obliquely oriented postvallid. Despite the odd occlusal plan of the talonid, the entoconid is situated directly lingual to the hypoconid,

placing it well mesial of the distolingual corner of the talonid. The entoconid gives rise to mesial (preentocristid) and distal crests. The former of these connects the entoconid with the lingual base of the postvallid, while the latter becomes confluent with the lingual end of the postcristid. The cristid obliqua is relatively straight, running mesially and lingually from the hypoconid to join the postvallid just lingual to the protoconid (in the holotype M_2). In DT1-41 the cristid obliqua climbs the postvallid to join the protocristid near its flexure, about midway between the protoconid and metaconid. The buccal cingulid is continuous on all lower molars, to the extent that the relevant anatomy is preserved.

M_3 is documented only by DT1-43 (Fig. 2f), the trigonid of which is missing. It has a distally extensive hypoconulid lobe, but otherwise resembles the more mesial molars in comparable parts.

The only upper tooth locus currently recognized for *K. arenula* is M^3, represented by DT1-37 (Fig. 2a). The crown as a whole is rhomboidal in occlusal outline, with relatively straight buccal and lingual margins matched by mesial and distal margins that are angled distolingually rather than being transverse. The paracone is significantly larger than the metacone, which is the chief reason why this tooth is identified as an M^3. The centrocrista is straight and mesiodistally oriented. Much shorter preparacrista and postmetacrista follow the same trajectory as the centrocrista. A small parastyle is present, and the buccal cingulum is continuous. The protocone is canted mesially. The pre- and postprotocristae are well-defined. The former structure runs from the protocone to the mesiobuccal corner of the tooth, being confluent with the precingulum. The postprotocrista runs buccally from the protocone up the

lingual face of the metacone. Conules are absent. There is a complete distal cingulum that is particularly extensive lingually, forming a small talon shelf. There is no appreciable development of a hypocone. Unlike the condition in *K. clarki*, the distal margin of the crown of M^3 is not invaginated.

Anthropoidea Mivart, 1864

Afrotarsiidae Ginsburg and Mein, 1987

Afrotarsius Simons and Bown, 1985

Afrotarsius libycus, sp. nov. (Fig. 2g-m)

Hypodigm. In addition to the holotype; DT1-31, right P^3; DT1-32, left P^3; DT1-33, left M^2; DT1-34, right M^2; DT1-36, right M_3.

Description. The holotype M_1 or M_2 (DT1-35) (Fig. 2k-l) cannot reliably be assigned to either tooth locus because these loci are virtually identical in the holotype lower jaw of *Afrotarsius chatrathi*[24]. The trigonid is appreciably narrower than the talonid. All three trigonid cusps are present, although the paraconid is shelf-like and integrated within its associated paracristid. The protoconid was apparently taller and more voluminous than the metaconid, although the apices of both the latter cusps are significantly worn. In occlusal view, the apices of the three trigonid cusps approximate the corners of an equilateral triangle. The metaconid is fully lingual in position, being situated slightly distally in relation to the protoconid. The buccal side of the protoconid is not perfectly vertical, so that the protoconid

occupies a less peripheral position on the trigonid than the metaconid. Although it is slightly obscured by wear, both of the latter cusps were connected by a protocristid that traversed the crown at a slightly oblique angle because of the relatively distal location of the metaconid noted earlier. The shelf-like paraconid is not fully lingual in position, but it is widely splayed with respect to the metaconid. The trigonid is broadly open lingually as a result. The talonid is evenly excavated and surrounded on all sides by cusps and crests. The hypoconid is the tallest talonid cusp, being situated at the distal end of the cristid obliqua. The latter structure is trenchant, running mesially and slightly lingually from the hypoconid to join the postvallid near the base of the protoconid. The entoconid lies directly lingual to the hypoconid, and an elevated preentocristid runs mesially from it to join the postvallid near the base of the metaconid. A small hypoconulid occurs midway between the hypoconid and entoconid, although it projects slightly distally in relation to both of the latter cusps. All three talonid cusps are joined by a well-developed postcristid that defines the distal extent of the talonid. A continuous cingulid lines the entire buccal margin of the tooth, extending distally from just below the paraconid to the buccal side of the hypoconulid.

M_3 (DT1-36) (Fig. 2m) bears the same basic molar morphology as the holotype, differing chiefly from it in the anatomy of the distolingual margin of the talonid. In contrast to the condition seen in the holotype M_1 or M_2, the entoconid of M_3 is reduced in size and its position is shifted somewhat buccally. The preentocristid is also less trenchant on M_3, so that the talonid is not as evenly excavated as it is in the holotype (being more nearly open lingually). As a result of the relatively buccal location of the entoconid, the highly reduced hypoconulid is located immediately adjacent to it. A similar condition occurs in the holotype of *Afrotarsius chatrathi*.

Two diminutive upper premolars are tentatively identified as left (DT1-32) (Fig.2j) and right (DT1-31) P^3 (Fig. 2i) of *Afrotarsius libycus*. Of the two specimens at hand, DT1-32 (Fig. 2j) is less worn, and the following description is based on this specimen. The buccal side of the tooth is dominated by the paracone, the apex of which is tilted slightly distally. The mesial side of the paracone is smoothly rounded and convex, while the distal side of the cusp bears a trenchant postparacrista that arcs distally and buccally before terminating at the distobuccal base of the crown. Minor breakage on the mesiobuccal margins of both specimens precludes determination of whether a small parastyle may have been present. The conical protocone is much smaller than the paracone and located near the center of the crown's lingual lobe. Pre- and postcingula frame the mesial and distal margins of the crown, but there is no lingual cingulum. A small postprotocrista runs distally from the apex of the protocone before becoming confluent with the postcingulum.

Two well-preserved upper molars are identified as left (DT1-33) (Fig. 2g) and right (DT1-34) (Fig. 2h) M^2 of *Afrotarsius libycus*. Although upper molars of *Afrotarsius* have not been described previously, we refer these specimens to *A. libycus* with confidence because they are appropriate in size and morphology to occlude with the holotype lower molar, and because they cannot be referred to any of the other primate taxa known from Dur At-Talah, each of which is also documented by upper molars that differ appreciably in morphology from that which is found here. DT1-33 is less worn than DT1-34, and the former specimen forms the basis for the following description. However, only minor morphological differences occur in the two specimens. Notable among these, DT1-34 has a more prominently invaginated ectoflexus and a more nearly continuous lingual cingulum than DT1-33. The buccal side of M^2 in *Afrotarsius* bears several features in common with Asian eosimiids, which is a primary

reason we assign *Afrotarsius* to the Anthropoidea. For example, both the paracone and metacone are located somewhat internally on the crown, because a well-developed buccal cingulum expands distally into a full-fledged shelf of enamel buccal to the metacone. The preparacrista and centrocrista are trenchant and oriented mesiodistally. In contrast, the postmetacrista forms an arcuate crest that runs distally and buccally from the metacone to terminate at a small metastyle near the distobuccal corner of the tooth. A minor swelling of enamel buccal to the mesial end of the preparacrista appears to mark the presence of a small parastyle. In addition to the mesial and distal crests that typically adorn the paracone and metacone on upper molars of Eocene primates, in *Afrotarsius* these cusps bear variably developed lingual crests that connect the apices of the paracone and metacone with their associated conules. Together with the relatively trenchant centrocrista and pre- and postprotocristae, these lingual crests from the paracone and metacone effectively surround the trigon with a virtually continuous series of crests. A very similar condition occurs on upper molars of Asian eosimiids, particularly *Bahinia pondaungensis*[5]. Conules are present, although these cuspules appear to be somewhat reduced in *Afrotarsius*. The paraconule is integrated into the preprotocrista, as is the metaconule with respect to the postprotocrista. Both conules give rise to pre- and postconule cristae. The preparaconule crista is confluent with the precingulum, while the postparaconule crista is confluent with the lingual crest from the paracone. A similar situation describes the relationships of the metaconule crista: the premetaconule crista is confluent with the lingual crest from the metacone, while the postmetaconule crista is confluent with the postcingulum. The protocone is tilted mesially, so that its apex lies nearer the paracone than the metacone. There is no development of a postprotocingulum. The mesial and distal margins of the protocone are lined by moderately developed cingula, but these structures fail to merge lingually.

Parapithecidae Schlosser, 1911

Biretia piveteaui de Bonis et al., 1988 (Fig. 2q-w)

Description. DT2-24 (Fig. 2u-v) is identified as M_2 rather than M_1 on the basis of its mesiodistally constricted trigonid and reduced paraconid, both of which are characters that distinguish these tooth loci in *Biretia fayumensis* and *B. megalopsis*[7]. DT2-24 is virtually identical to the holotype of *Biretia piveteaui* from Bir El Ater, Algeria[6]. The trigonid is dominated by the protoconid, which is substantially taller and more voluminous than the metaconid, as is typical in basal anthropoids[12]. The preprotocristid is poorly developed, extending a short distance down the mesial face of the protoconid before angling sharply lingually to merge with the paracristid. The diminutive paraconid is integrated within the weak paracristid. The paraconid is not fully lingual in position, being located mesially and slightly buccally with respect to the metaconid. A minor difference between DT2-24 and the holotype of *Biretia piveteaui* concerns the relationship between the paraconid and metaconid on M_2. In DT2-24 these two cusps are separated by a tiny furrow, while in the holotype of *Biretia piveteaui* they are connected by a weak premetacristid that is lacking in DT2-24. The protocristid is obliquely oriented because the metaconid is situated slightly distally with respect to the protoconid. All three talonid cusps are well defined and relatively bulbous, with the hypoconid being the largest. The hypoconulid is central in position, and the entoconid is located slightly forward of the distolingual corner of the talonid, leaving space for a tiny distolingual fovea. The cristid obliqua is not particularly trenchant, but it is present, in contrast to the condition in *Qatrania* (including *Abuqatrania*), in which this crest is greatly reduced or even lost. Likewise, a short preentocristid connects the entoconid with the base of the postvallid, and minor crests connect the entoconid and hypoconid with the hypoconulid. All of these talonid crests are more or less suppressed in *Qatrania*. *Biretia fayumensis* and *B.*

megalopsis from the BQ-2 locality in the Fayum[7] resemble *Qatrania* and differ from *Biretia piveteaui* in having weaker (or even lacking altogether) talonid crests linking the hypoconulid with the entoconid and hypoconid. As a result, the distolingual fovea is larger in Fayum species of *Biretia* (particularly *B. megalopsis*) than is the case in *B. piveteaui*.

DT1-29 (Fig. 2w) is a left M_3. It bears the same general molar morphology as DT2-24, with the most important differences being talonid structure. The talonid of M_3 is narrower than the trigonid, which is not the case for M_2. The hypoconulid extends somewhat distally beyond the remainder of the talonid, as is typical for early primates. However, this distal extension is much less than that which typically occurs among Eocene primates other than anthropoids. The hypoconulid of M_3 is slightly larger and more distally extensive in *Biretia piveteaui* than it is in *B. megalopsis*. In this respect, *B. piveteaui* more closely resembles *B. fayumensis*.

DT1-26 (Fig. 2t) is a left M^1 of *B. piveteaui*. Its crown is bunodont and the major cusps are inflated. The paracone and metacone are similar in size and situated near the buccal margin of the crown. There is no buccal cingulum. The preparacrista, centrocrista, and postmetacrista are aligned mesiodistally. A tiny parastyle occurs at the mesial end of the preparacrista, but there is no metastyle. The protocone and hypocone are similar in size, and these lingual cusps are situated almost directly opposite the paracone and metacone, respectively. As a result, the crown has a very quadrate appearance in occlusal view. The hypocone is considerably larger and more inflated than is the case in *B. fayumensis*. A very short, poorly developed preprotocrista unites the apex of the protocone with the well-developed, bulbous paraconule. A weak preparaconule crista continues mesiobuccally from the paraconule to become confluent with the precingulum. There is no postparaconule crista. The bulbous metaconule lacks any associated cristae, and it is not connected to the protocone because of the absence of a postprotocrista. As a result, both upper molar conules, particularly

the metaconule, are relatively isolated in *B. piveteaui*. In Fayum species of *Biretia* the upper molar metaconules are less isolated, because the postprotocrista and postmetaconule crista are retained, yet weakly developed. A small mesial cingulum runs from below the paraconule to the base of the protocone. A much broader distolingual cingulum supports the massive hypocone, but the mesial and distal cingula fail to unite lingual to the protocone.

DT1-27 (Fig. 2s) is a right M^2 of *B. piveteaui* missing the distobuccal part of the crown. It is virtually identical in morphology to M^1, differing chiefly in being relatively shorter and broader (i.e., more transverse) in occlusal outline. It also differs from M^1 in having a complete lingual cingulum. *B. piveteaui* lacks any development of a pericone on M^{1-2}.

Two examples of M^3 are available, DT1-28 (Fig. 2r) and DT2-23 (Fig. 2q), both of which come from the right side. DT2-23 is virtually pristine, while much of the enamel has been etched away from DT1-28. Accordingly, the following description is based on the former specimen. The crown as a whole is oval in occlusal outline, being much broader transversely than it is long. The paracone is significantly larger than the vestigial metacone. The buccal crests run mesiodistally, although the postmetacrista is absent owing to the extreme reduction of the metacone. A mesial cingulum is well-developed, being confluent buccally with the preprotocrista. Conules are absent. A lingual crest arises from the apex of the paracone, connecting that cusp with the protocone on its way to join the complete lingual cingulum. The postcingulum forms a shelf-like structure that is buccally continuous with the reduced metacone. The trigon as a whole is reduced, sloping distally.

Oligopithecidae Simons, 1989

Talahpithecus parvus, gen. et sp. nov. (Fig. 2n-p)

Hypodigm. In addition to the holotype; DT1-30, right P^4; DT1-32, right M_1 or M_2.

Description. DT1-32 (Fig. 2p) is a right M_1 or M_2 that unfortunately is missing the mesial part of its trigonid. The poorly preserved postcristid appears to have been oriented almost directly transversely. If so, this tooth more likely represents M_2 than M_1, because the postvallid is more obliquely oriented on M_1 in *Catopithecus*. The trigonid is relatively taller and the postvallid is more nearly vertical in *Talahpithecus* than is the case in *Catopithecus* and *Oligopithecus*. Talonid proportions are also longer and narrower than in younger oligopithecids. As a result, the talonid basin in *Talahpithecus* is clearly longer than it is wide, whereas the reverse is true in *Catopithecus* and *Oligopithecus*. The entoconid in DT1-32 is elevated above the adjacent part of the talonid, and a distinct preentocristid connects the entoconid to the lingual base of the postvallid. This condition differs from that which occurs in lower molars of *Catopithecus* and *Oligopithecus*, in which the preentocristid is greatly reduced or absent, yielding a talonid that is nearly open lingually between the entoconid and postvallid. The hypoconulid is smaller than either the entoconid or the hypoconid, and it is situated near the distolingual corner of the talonid, immediately adjacent to the entoconid (as is typical of oligopithecids). The hypoconid is large and angular. The cristid obliqua is trenchant, and it runs straight from the hypoconid to the base of the protoconid. As a result, the hypoflexid is very shallow. A weak postcristid connects the hypoconid with the hypoconulid, but this crest is so low that the talonid is nearly open distally.

DT1-30 (Fig. 2o), a fragmentary right P^4, is broken distolingually. The buccal margin of the tooth is dominated by the tall, distally tilted paracone. Well-defined pre- and postparacristae emerge from the apex of the paracone, and these are mesiodistally aligned. The preparacrista is noticeably longer than the postparacrista owing to the distal orientation of the paracone noted earlier, as well as the elevated distobuccal corner of the crown. A buccal cingulum is present and continuous. The much smaller protocone lies near the mesiolingual

margin of the crown. Weak crests run mesiobuccally and distally from the apex of the protocone to join the continuous pre- and postcingulum, respectively.

The holotype left M^1 or M^2 (DT1-31) (Fig. 2n) is well-preserved aside from minor damage to the paracone and the distolingual cingulum. The crown bears three main cusps that are similar in size. The paracone and metacone are located near the buccal periphery of the crown. There is no buccal cingulum. The centrocrista is straight, mesiodistally oriented, and trenchant. Much shorter preparacrista and postmetacrista follow the same general trajectory as the centrocrista, although the postmetacrista deviates slightly buccally as it approaches the distobuccal margin of the crown. A small parastyle occurs at the mesiobuccal margin of the crown, but there is no clear metastyle. The protocone is tall and mesially canted, so that its apex lies nearer the paracone than the metacone. Trenchant pre- and postprotocristae delimit the lingual margin of the trigon. These crests continue buccally beyond the location where conules would normally occur (these are absent) to merge with lingual crests that arise from the apices of the paracone and metacone. As a result, the trigon is completely surrounded by trenchant crests. Where a paraconule would normally occur, the preprotocrista divides into two branches. The more mesial branch continues mesiobuccally to form a short precingulum, whereas the other branch climbs the lingual face of the paracone as noted earlier. The lingual cingulum is complete and well-defined. A tiny swelling of enamel marks an incipient pericone located directly lingual to the protocone. A tiny crest runs from the pericone part way up the lingual face of the protocone. There is no clear evidence of a distinct hypocone, although minor damage to the distolingual cingulum may have obscured the presence of this structure. The lingual cingulum is continuous on either side with mesial and distal cingula, the latter of which is more buccally extensive.

Supplementary Table 1. Metric data (in mm) for fossil primate teeth from the Dur At-Talah fauna of central Libya. For lower molars, "width" corresponds to trigonid width. Asterisks indicate estimated measurements of fragmentary specimens.

Taxon	Specimen #	Tooth locus	Length	Width	Talonid width
Karanisia arenula	DT1-37	M^3	1.97	2.70	
Karanisia arenula	DT1-38	P_3	1.63	1.19	
Karanisia arenula	DT1-39	P_4	2.46		1.31
Karanisia arenula	DT1-40	M_1	2.48	1.53	
Karanisia arenula	DT1-41	M_1	2.52	1.44	
Karanisia arenula	DT1-42	M_2	2.48	1.74	1.57
Karanisia arenula	DT1-43	M_3	2.98*		1.60
Afrotarsius libycus	DT1-31	P^3	1.07	1.64	
Afrotarsius libycus	DT1-32	P^3	1.12	1.62	
Afrotarsius libycus	DT1-33	M^2	2.25	3.26	
Afrotarsius libycus	DT1-34	M^2	2.32	3.26	
Afrotarsius libycus	DT1-35	M_1 or M_2	2.22	1.50	1.66
Afrotarsius libycus	DT1-36	M_3	2.27	1.34	1.27
Biretia piveteaui	DT1-26	M^1	2.65	3.36	
Biretia piveteaui	DT1-27	M^2	2.50	3.68	
Biretia piveteaui	DT1-28	M^3	1.53	3.17	
Biretia piveteaui	DT2-23	M^3	1.40	2.65	
Biretia piveteaui	DT2-24	M_2	2.66	2.18	1.97
Biretia piveteaui	DT1-29	M_3	2.49	1.65	1.36
Talahpithecus parvus	DT1-30	P^4	2.15	2.72	

Talahpithecus parvus	DT1-31	M^1 or M^2	2.82	3.40	
Talahpithecus parvus	DT1-32	M_1 or M_2	2.59*	1.94	1.92